AMERICAN SOCIETY FOR MICROBIOLOGY | mBio®

RESEARCH ARTICLE
Host-Microbe Biology

Gut Microbial and Metabolic Responses to *Salmonella enterica* Serovar Typhimurium and *Candida albicans*

Jennifer R. Bratburd,[a] Caitlin Keller,[b] Eugenio Vivas,[a] Erin Gemperline,[b]* Lingjun Li,[b,c] Federico E. Rey,[a] Cameron R. Currie[a]

[a]Department of Bacteriology, University of Wisconsin, Madison, Wisconsin, USA
[b]Department of Chemistry, University of Wisconsin, Madison, Wisconsin, USA
[c]School of Pharmacy, University of Wisconsin, Madison, Wisconsin, USA

ABSTRACT The gut microbiota confers resistance to pathogens of the intestinal ecosystem, yet the dynamics of pathogen-microbiome interactions and the metabolites involved in this process remain largely unknown. Here, we use gnotobiotic mice infected with the virulent pathogen *Salmonella enterica* serovar Typhimurium or the opportunistic pathogen *Candida albicans* in combination with metagenomics and discovery metabolomics to identify changes in the community and metabolome during infection. To isolate the role of the microbiota in response to pathogens, we compared mice monocolonized with the pathogen, uninfected mice "humanized" with a synthetic human microbiome, or infected humanized mice. In *Salmonella*-infected mice, by 3 days into infection, microbiome community structure and function changed substantially, with a rise in *Enterobacteriaceae* strains and a reduction in biosynthetic gene cluster potential. In contrast, *Candida*-infected mice had few microbiome changes. The LC-MS metabolomic fingerprint of the cecum differed between mice monocolonized with either pathogen and humanized infected mice. Specifically, we identified an increase in glutathione disulfide, glutathione cysteine disulfide, inosine 5′-monophosphate, and hydroxybutyrylcarnitine in mice infected with *Salmonella* in contrast to uninfected mice and mice monocolonized with *Salmonella*. These metabolites potentially play a role in pathogen-induced oxidative stress. These results provide insight into how the microbiota community members interact with each other and with pathogens on a metabolic level.

IMPORTANCE The gut microbiota is increasingly recognized for playing a critical role in human health and disease, especially in conferring resistance to both virulent pathogens such as *Salmonella*, which infects 1.2 million people in the United States every year (E. Scallan, R. M. Hoekstra, F. J. Angulo, R. V. Tauxe, et al., Emerg Infect Dis 17:7–15, 2011, https://doi.org/10.3201/eid1701.P11101), and opportunistic pathogens like *Candida*, which causes an estimated 46,000 cases of invasive candidiasis each year in the United States (Centers for Disease Control and Prevention, *Antibiotic Resistance Threats in the United States, 2013*, 2013). Using a gnotobiotic mouse model, we investigate potential changes in gut microbial community structure and function during infection using metagenomics and metabolomics. We observe that changes in the community and in biosynthetic gene cluster potential occur within 3 days for the virulent *Salmonella enterica* serovar Typhimurium, but there are minimal changes with a poorly colonizing *Candida albicans*. In addition, the metabolome shifts depending on infection status, including changes in glutathione metabolites in response to *Salmonella* infection, potentially in response to host oxidative stress.

KEYWORDS *Salmonella*, gut microbiome, metabolomics, metagenomics

Symbiotic microbes help shape the biology of plants and animals (1). In humans, gut microbes modulate nutrition and immune function and are correlated with an increasing number of metabolic and neurological health and disease states (2, 3). The

Received 21 September 2018 **Accepted** 27 September 2018 **Published** 6 November 2018

Citation Bratburd JR, Keller C, Vivas E, Gemperline E, Li L, Rey FE, Currie CR. 2018. Gut microbial and metabolic responses to *Salmonella enterica* serovar Typhimurium and *Candida albicans*. mBio 9:e02032-18. https://doi.org/10.1128/mBio.02032-18.

Editor Martin J. Blaser, New York University

Address correspondence to Lingjun Li, lingjun.li@wisc.edu, Federico E. Rey, ferey@wisc.edu, or Cameron R. Currie, currie@bact.wisc.edu.

* Present address: Erin Gemperline, Dow AgroSciences, Indianapolis, Indiana, USA.

J.R.B. and C.K. contributed equally to this work.

This article is a direct contribution from a Fellow of the American Academy of Microbiology. Solicited external reviewers: Ansel Hsiao, University of California, Riverside; Katrine Whiteson, University of California, Irvine.

human gastrointestinal tract harbors the largest fraction of microbial life in the body, estimated to range from 10^8 to 10^{10} bacteria per gram in the ileum and stool, respectively (4). Bacteria are the dominant taxa in the human gut microbiome, with the most abundant lineages belonging to the phyla *Bacteroidetes* and *Firmicutes*. Nevertheless, these communities are highly diverse and include viruses, archaea, fungi, and protists (5–8), and all combined contain 150 times as many genes as the human genome (9). In a healthy state, the human gut microbiome is relatively stable over time (10, 11). Major disruption of the gut microbiome is associated with infections by a number of serious human pathogens, such as *Clostridium difficile,* vancomycin-resistant *Enterococcus* (VRE), and *Salmonella enterica* (12–14).

Preventing exogenous microbes from colonizing the human intestine is critical to the host maintaining a stable and healthy gut microbiome. The role of the microbiome in preventing pathogens from invading the gut has been recognized since the 1950s, when pretreatment with antibiotics was shown to drop the infectious dose of *Salmonella enterica* 100,000-fold (15). Gut microbes confer colonization resistance by outcompeting pathogens for nutrients, priming the host immune system, and directly targeting other microbes with metabolites (16). Several examples of metabolites produced or modified by the microbiota that inhibit pathogens include short-chain fatty acids, secondary bile acids, and modified compounds from the diet (17–19). In addition, some members of the microbiota can create compounds to respond selectively to pathogen infection (20). The gut microbiota has the potential to make a wide variety of novel natural products, and many of the large biosynthetic gene clusters encoding natural products are found in relatively small genomes, indicative of an ecological role for the products (21).

Experiments using gnotobiotic mice with and without human microbiota, in combination with metagenomic and metabolomic approaches, can provide insight on the structure and function of the gut microbiota during pathogen invasion. Gnotobiotic mice are a mammalian model system in which defined microbiomes can be used in a controlled environment. Various metabolomics techniques, including nuclear magnetic resonance and chromatography-mass spectrometry, have been used for large-scale characterization of metabolite changes as a result of microbiome colonization, illustrating the impact of the microbiota on not only intestinal metabolism but also global systems (22, 23). Furthermore, liquid chromatography-mass spectrometry (LC-MS) can help to characterize metabolite changes due to disturbances in the microbiome (24, 25) and to screen for novel secondary metabolites and natural products in bacterial systems (26, 27).

Here we examine colonization resistance in the humanized (HUM) mouse model. Specifically, we perform experimental infection with *Salmonella enterica* serovar Typhimurium and *Candida albicans* in HUM mice and in germfree (GF) mice. *Salmonella enterica* Typhimurium is a disruptive pathogen that causes massive inflammation to outcompete the native microbiota in mice and human models (28–30). *Candida albicans* can cause low-grade inflammation, but in contrast to *Salmonella enterica* Typhimurium is considered a commensal and occasional opportunistic pathogen in the GI tract (31–34). Nevertheless, *C. albicans* has been shown to colonize GF and antibiotic-treated adult mice (33, 35, 36), which appear otherwise resistant, suggesting that gut microbiota play a role in preventing *Candida* colonization in mice and humans. In this study, we investigate how these pathogens alter the structure of the human gut microbiome, the biosynthetic gene cluster potential, and the metabolites produced in a healthy or infected state. We cross the presence and absence of the microbiome with the presence and absence of pathogen infection, using either *S. enterica* Typhimurium or *C. albicans*. To characterize strain-level diversity that is not resolvable with 16S rRNA gene sequencing, we use shotgun metagenomics on fecal samples over 3 days of infection. We also identify the capacity of community members to produce novel antimicrobials through the biosynthetic gene clusters embedded in bacterial genomes. Further, we characterize metabolites using LC-MS for relative quantification and dis-

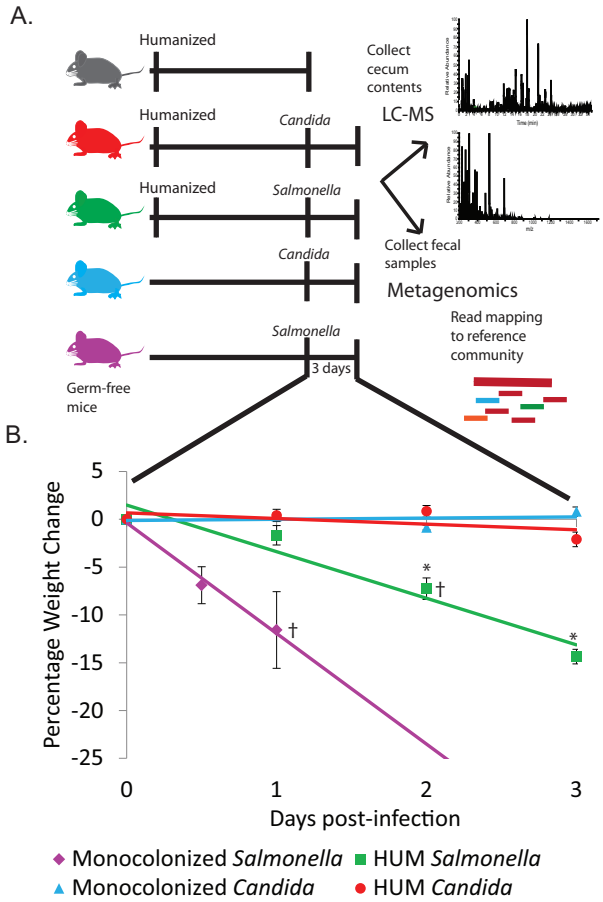

FIG 1 (A) Overview of experimental design. (B) Percent body weight loss during 3 days of infection. Errors bars indicate standard error. Significant difference from HUM *Candida* ($P < 0.05$) using Wilcoxon test denoted by * next to relevant group. Mice sacrificed early indicated with † (monocolonized *Salmonella*, 3 at 12 h and 3 at 24 h, HUM *Salmonella* 1 at 24 h).

covery metabolomics in the host cecum during infection and validate the identifications of several specific metabolites with commercial standards.

RESULTS

Infection severity in mice with and without microbiota. Germfree mice, 8 to 12 weeks old, were kept germfree or colonized via oral gavage with a synthetic human community for 2 weeks, and then infected with *Salmonella enterica* Typhimurium or *Candida albicans* (Fig. 1A). All infected mice showed presence of pathogens in fecal samples by growth on selective media. Prior to infection, the mice weighed on average 29.8 g ± 2.3 (mean ± SD). GF mice infected with *Salmonella* ($n = 6$), henceforth referred to as monocolonized *Salmonella* mice, lost an average body mass of 2.0 ± 1.4 g or 6.8% ± 4.7% within 12 h postinfection. Due to severity of symptoms, three monocolonized *Salmonella* mice were sacrificed 12 h postinfection, and the remaining monocolonized *Salmonella* mice and one HUM mouse infected with *Salmonella* were sacrificed within 24 h of infection. HUM mice infected with *Salmonella* surviving 3 days into infection ($n = 5$) lost an average of 4.2 ± 0.6 g or 14.3% ± 1.7%, a significant loss in comparison to weight change from both the monocolonized and HUM mice infected with *Candida* (Mann-Whitney U test, Bonferroni corrected, $P < 0.05$). The monocolonized *Candida* mice ($n = 6$) gained on average 0.2 ± 0.3 g or 0.8% ± 1.1% of their original weight, and the *Candida*-infected HUM mice ($n = 6$) gained on average 0.7 ± 0.5 g or 2.0% ± 1.8% of their original weight. There was no statistically significant

difference in the change in weight for the monocolonized *Candida* mice compared to the HUM mice infected with *Candida* by the endpoint of the experiment, 3 days of infection.

Microbial community shifts in response to infection. We conducted Illumina-based metagenomic sequencing on DNA from fecal pellets collected throughout infection. Each sample had on average 407,535 reads (SD = 63,381), ranging from 295,235 to 523,271 reads. The average number of reads with at least one reported alignment was 385,882 ± 96,477, or 95% of reads per sample. Prior to infection, the most abundant strains, making up over half of the relative abundance in the metagenomes from all groups, were *Bacteroides cellulosilyticus* DSM14838, *Subdoligranulum variabile*, *Bacteroides cellulosilyticus* WH2, *Akkermansia muciniphila*, and *Clostridium bolteae* with an average relative abundance of 15.1%, 14.1%, 9.1%, 7.8%, and 6.5%, respectively (Fig. 2A). By day three in the *Salmonella*-infected HUM mice, most of the communities were dominated by *Salmonella* and other various *Enterobacteriaceae* strains from the original inoculum. Furthermore, diversity significantly decreased in *Salmonella*-infected mice (see Fig. S1 in the supplemental material). Prior to infection, these strains (*C. youngae*, *P. penneri*, *E. cancerogenus*, and *E. fergusonii*) in total represented an average relative abundance of 0.2%. In the metagenomes from two mice, we observed an increase in the reads mapping to *Enterobacter cancerogenus*, up to 26.4% and 26.6% of the community, along with a smaller increase in *Proteus penneri*. One mouse had an increase in *Escherichia fergusonii* to 22.9% of the metagenome, while it remained below 1% of the metagenome in all the other mice. In another mouse, *Citrobacter youngae* reads increased to 15.2%, while in other mice *C. youngae* reads remained below 7.9%. After excluding *Salmonella* reads, we continued to observe a large shift in the relative abundance of community members. Using principal component analysis (PCA), we show large separation of the HUM *Salmonella* microbiome communities, 3 days postinfection, from a tight cluster of all other time points and treatments, with the first component explaining 31.4% of the variation (Fig. 2B).

In all *Candida*-infected HUM mice, less than 1% of reads mapped to the *Candida albicans* SC5314 reference genome. The metagenome of this group was not significantly different from uninfected HUM mice. The community structure remained fairly consistent over the infection period, although there was some variation in strain relative abundance over time (Fig. 2). The largest change in any individual strain's relative abundance was an 8.4% increase in *Subdoligranulum variabile* in one mouse from 1 day postinfection to 3 days postinfection.

Prevalence of biosynthetic gene clusters within genomes and metagenomes. In total, from the genomes of the human microbiome used in this study, using antiSMASH 4.0 (37), we detected 1,081 biosynthetic gene clusters (BGCs). Of these clusters, when grouped together using BiG-SCAPE with a cutoff distance of 30 calculated based on a weighted combination of Jaccard, domain sequence similarity, and adjacency index, we identified 128 cluster nodes in 51 groups. The remaining 953 BGCs did not form any groupings with each other. Based on antiSMASH-predicted classifications, most clusters were classified as other, which included putative clusters (486), fatty acids (117), fatty acid-saccharide combined clusters (22), aryl polyenes (14), siderophores (4), and resorcinol (3). Another large category was saccharides (345), followed by 62 ribosomally synthesized and posttranslationally modified peptides (RiPPs), a group that includes bacteriocins, sactipeptides, lantipeptides, and thiopeptides. We also found 20 nonribosomally synthesized peptide clusters and one hybrid polyketide-NRPS cluster in *Desulfovibrio piger* (Table S1).

We found significant differences in the percentages of total metagenomic reads mapping to BGCs in *Salmonella*-infected HUM mice prior to infection versus 3 days postinfection (Wilcoxon $P < 0.05$, corrected with Benjamini-Hochberg), excluding reads mapping to BGCs from *Salmonella* itself. Saccharides, lantipeptides, aryl polyenes, sactipeptides, fatty acids, fatty acid-saccharides, terpenes, and putative clusters were significantly reduced, while thiopeptides significantly increased 3 days postinfection

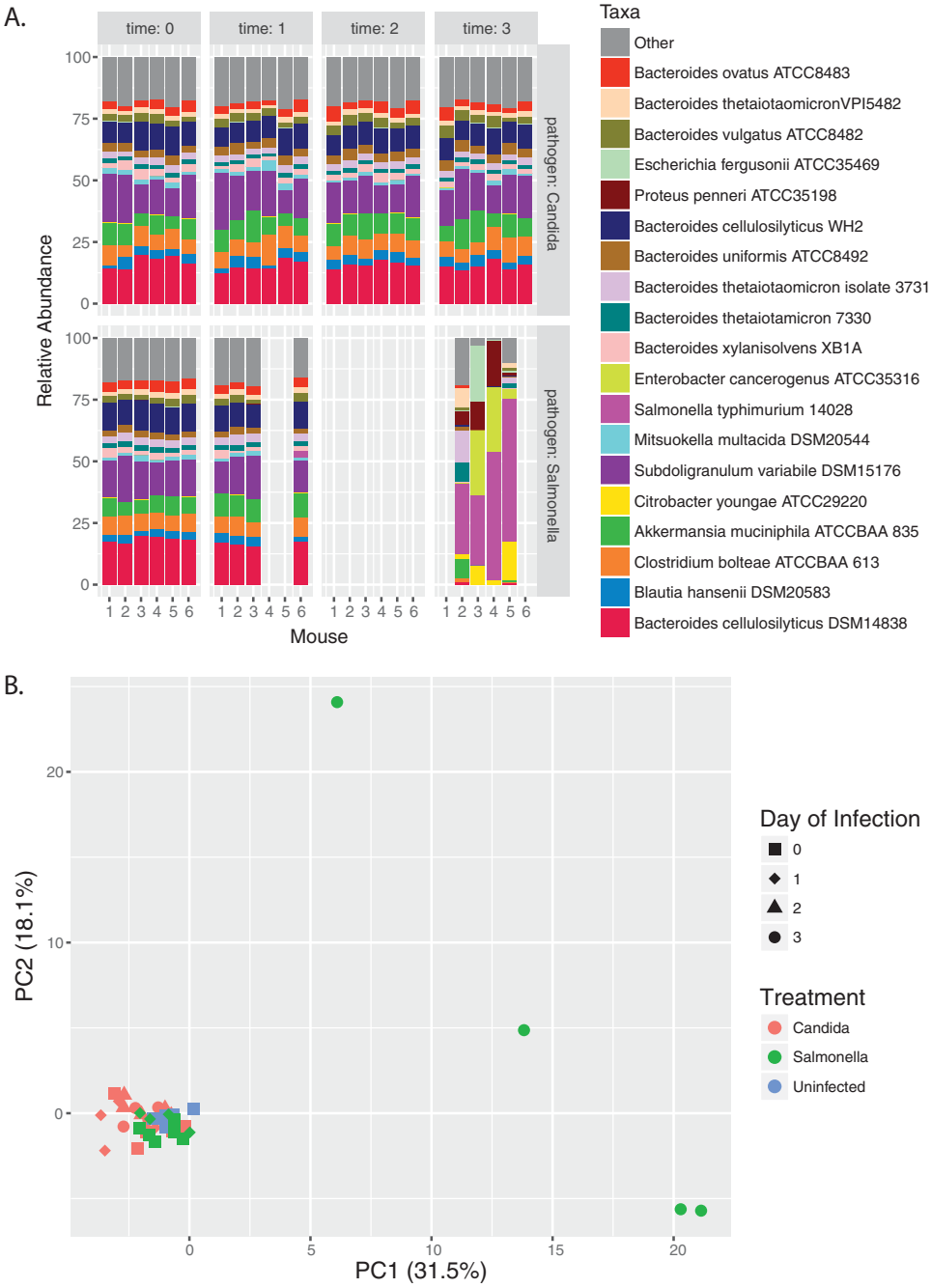

FIG 2 Variation in fecal microbiota metagenomes during infection. (A) Relative abundance of top 19 strains in HUM *Candida albicans* and *Salmonella enterica* Typhimurium infection group. (B) PCA of strain relative abundance.

(Fig. 3). The majority of non-*Salmonella* reads mapping to thiopeptide clusters mapped to *Citrobacter youngae*, *Enterobacter cancerogenus*, *Proteus penneri*, and *Escherichia fergusonii*, consistent with the overall increase relative abundance in *Enterobacteriaceae* described above.

Differential metabolomics during infection and novel metabolite potential. Analysis of the LC-MS results with Compound Discoverer (Thermo Fisher Scientific) resulted in the grouping of 8,613 merged features (chromatographic peaks) into 8,259 putative compounds. The compounds detected from the cecum samples of one or more mice from each treatment group totaled 3,254 for the monocolonized *Candida* mice, 3,696 compounds for the monocolonized *Salmonella* mice, 3,349 compounds for

FIG 3 Percent abundance of reads mapping to biosynthetic gene clusters out of total reads that were mapped from the metagenome from HUM *Salmonella*-infected mice prior to infection ($n = 6$) and 3 days into infection ($n = 4$), on a square root-adjusted axis. Significance ($P < 0.05$ with Benjamini-Hochberg correction) is indicated with *.

the uninfected HUM mice, 2,924 compounds for the HUM mice infected with *Candida*, and 2,815 compounds for the HUM mice infected with *Salmonella*.

LC-MS *m/z* values and relative intensities from cecum contents showed separation of samples with PCA. Two components were able to explain 67.7% of the variance (Fig. S2). Using partial least-squares discriminant analysis (PLS-DA), we observed distinct separation of all groups with two components (R2 = 0.70799, Q2 = 0.66183 for component 1 and R2 = 0.85972 and Q2 = 0.81188 for component 2; Fig. 4A). Using permutation testing of the PLS-DA, we obtained statistical significance ($P < 0.001$) for 1,000 permutations. The outliers in the *Salmonella*-infected HUM mouse group were from two technical replicates of one sample that had to be sacrificed 24 h into infection. We also found distinct patterns for different groups of metabolites (Fig. 4B), which indicate similar patterns between uninfected HUM and *Candida*-infected HUM mice compared to monocolonized infected mice and HUM *Salmonella* mice. Additionally, we identified numerous features overrepresented in the monocolonized groups compared to the HUM groups (Fig. S3).

To examine metabolites potentially produced by the microbiome in response to infection, we looked for metabolites that were typically not found in pathogen-monocolonized mice (absent in at least 8 of 12 samples, representing 6 biological replicates with 2 technical replicates each) and were at least 1.5-fold higher in abundance in infected HUM mice compared to the highest normalized area of the controls (HUM mice with no infection). Using these guidelines, we narrowed our metabolites of interest to 31 out of 8,085 features detected overall. We detected 22 features in higher abundance in HUM *Salmonella*-infected mice. In HUM *Candida*-infected mice, we found 10 features of interest based on the above criteria. One metabolite (*m/z* 347.0626, retention time 1.05 min) appeared to be shared between the lists, and also had matching tandem MS fragmentation from both infection groups. This metabolite had similar MS/MS to 3′AMP and 2′AMP standards, but the experimental retention time did not match that of the standards (1.37 min for 3′AMP and 2.22 min for 2′AMP). From the 31 selected compounds of interest, only 6 from HUM *Salmonella* and 4 from *Candida* infection had putative identifications based upon accurate mass matching to KEGG, HMDB, or AntiBase, leaving a remaining total of 21 potentially novel compounds (Table S2). *In silico* fragmentation with MetFrag (38) was performed using MS/MS spectra obtained on the targets. If the top peaks in the experimental MS/MS were

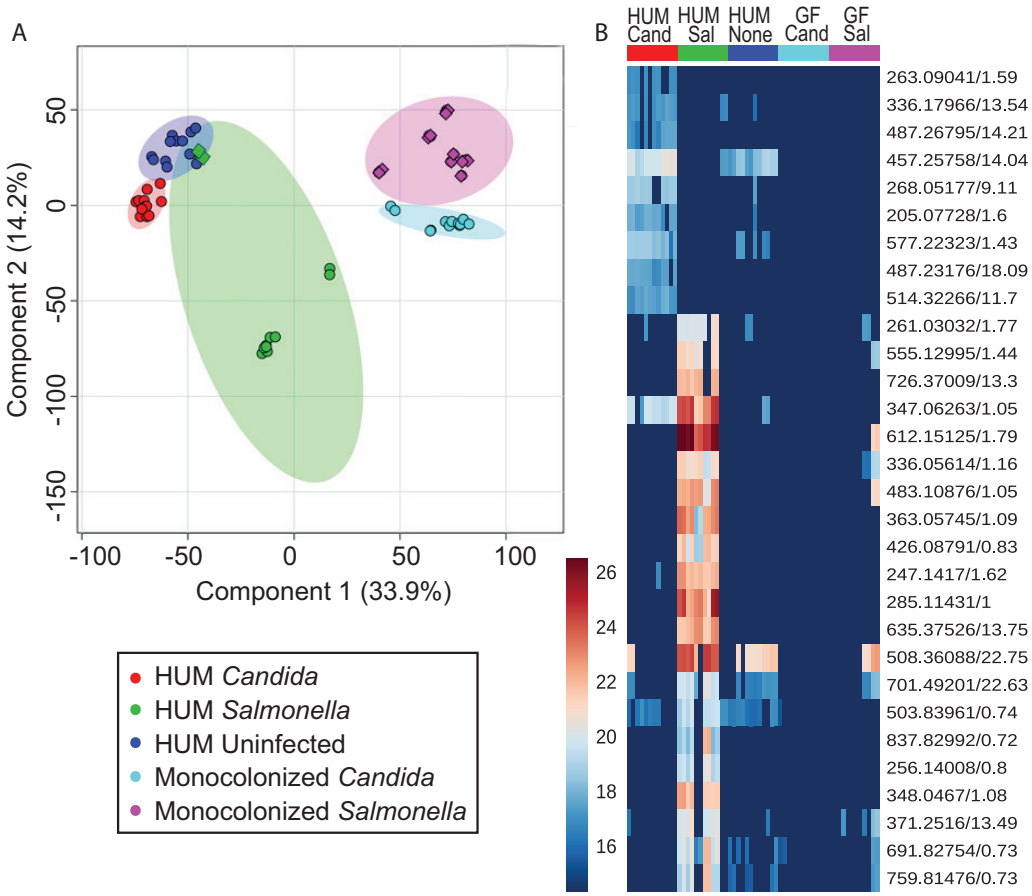

FIG 4 (A) PLS-DA of metabolites from all groups, with 95% confidence intervals. (B) Metabolites of interest 1.5× higher in HUM infected groups than uninfected mice, absent in 8/10 technical replicates for monocolonized mice. Circles are samples collected three days postinfection; diamonds are from animals sacrificed 1 day postinfection.

explained by the *in silico* fragmentation, then standards were obtained to confirm the identification. Using this procedure, we identified glutathione disulfide, glutathione cysteine disulfide, inosine 5′-monophosphate, and hydroxybutyrylcarnitine as compounds upregulated from the HUM *Salmonella* group (Fig. S4). Although the *in silico* fragmentation approach worked well for the targets with KEGG matches, the increasing number of compounds in the more inclusive databases made it difficult to find putative identifications with MS/MS for targets that did not have matches to the KEGG databases.

DISCUSSION

Understanding how microbial communities change in response to perturbation is crucial for health, not only because the microbiota can protect the host against pathogenic microbes but also because changes in the gut microbiota have been associated with multiple health conditions (39). Increasingly it has been recognized that pathogenicity and virulence can depend on the context of specific microbe-microbe interactions or the whole community, indicating the importance of studying pathogen-microbiome interactions (40, 41). In this study, we compare how two pathogenic perturbations affect the structure and function of human gut microbiota in a gnotobiotic mouse model. We find that during infection with *Salmonella*, the structure and functional capacity of the microbiota change. Corresponding to these changes, we see significant changes in metabolites before versus during infection that vary with and without the human microbiota.

Our infection experiments revealed significant differences among treatments as

measured by weight loss. *Candida*-infected mice had weights that remained around their baseline starting weight. While we did isolate CFUs of *Candida* from mouse feces using media with antibiotics, indicating that viable yeast cells passed through the host, reads mapping to *Candida* from the metagenomic data were at or below the limit of detection, suggesting that *Candida* did not readily colonize these mice. Alternatively, the lack of fungal DNA may be influenced by our DNA extraction method (42). In contrast, *Salmonella*-infected mice lost significantly more weight than *Candida*-infected mice by 3 days into infection, regardless of microbiome presence or absence. GF mice infected with *Salmonella* were moribund within 24 h, while HUM mice infected with *Salmonella* were able to survive until the end of the 3 days, with the exception of one mouse, indicative of the protective effects of the microbiota against *Salmonella*.

Salmonella infection perturbed the microbiota and led to an increase in the relative abundance of different *Enterobacteriaceae*, whereas *Candida* did not. Prior to infection, the microbiota contained similar dominant taxa including *Bacteroidetes* and *Firmicutes* with relatively few *Gammaproteobacteria*. During *Salmonella* infection in humanized mice, the metagenomic data indicated an increase in the relative abundance of *Enterobacteriaceae* (including strains besides *Salmonella*). This result is consistent with previous work examining changes in gut microbial communities during *Salmonella* infection (28, 43, 44), and resembles increases in *Enterobacteriaceae* during antibiotic treatment (13), both of which may ultimately be driven by the oxygenation of the gut (45). These changes may represent a bloom of closely related strains or a reduction in the size of the bacterial community overall. Although *Enterobacteriaceae* increased in the samples, which particular strains increased appeared stochastic. Some of the variation may be due to read mapping of conserved genes to closely related strains; however, we saw similar results using different read mapping programs (Bowtie and Burrows-Wheeler Algorithm) and using parameters to exclude non-uniquely mapping reads. Given that these strains may compete with *Salmonella* over electron acceptors and trace elements, further investigation on these dynamic interactions is warranted (46, 47). The stochasticity may also reflect the general instability of the community. While *Salmonella* dramatically perturbs the community, *Candida* did not seem to readily colonize the mice, and although some changes occurred in the microbial communities, these fluctuations are within the range of natural variation.

The synthetic human microbiome used in this study contained many biosynthetic gene clusters, and the potential functional capacity changed with infection treatment. In our input strains we found potential for unknown biosynthetic gene clusters, including RiPPs, NRPS clusters, and many putative clusters. This fits with previous observations; biosynthetic gene clusters are common in human gut microbiota and anaerobic bacteria (21, 48). Metagenomic analysis indicated a decrease in most cluster types during *Salmonella* infection, which likely reflects a drop in community diversity. One exception was the increase in reads mapping to gene clusters involved in thiopeptide biosynthesis, which was increased even after removing reads mapping to *Salmonella*'s own thiopeptide biosynthesis cluster. Thiopeptides are a class of peptide antibiotics that target Gram-positive bacteria (49). Since *Salmonella* is Gram-negative and has one putative thiopeptide BGC of its own, it seems unlikely that these thiopeptide clusters, if produced, would target *Salmonella*. Other possibilities are that if produced, these secondary metabolites encoded by clusters might add to the community instability, or that these genes are not transcribed or translated. Alternatively, this result may suggest that the pathogen-induced disruption in the microbiome helps diminish members that would have been capable of producing BGC products. Further research will be needed to characterize what role, if any, these BGCs play during infection.

Our discovery metabolomics showed differences in the metabolites present in the mouse cecum based on presence of microbiome as well as infection. For example, the metabolomes of *Salmonella*-infected, *Candida*-infected, and uninfected mouse ceca grouped separately on PLS-DA analysis, suggesting distinct metabolic responses between a virulent bacterial pathogen and opportunistic fungal pathogen. The changes

in overall metabolites based on gut microbiota support previous research comparing germfree and colonized mice and mice with different gut microbiome donors (50). We found more putative metabolites of interest (based on higher abundance in HUM infected mice and generally absent in GF mice) from *Salmonella*-infected mice than *Candida*-infected mice. Previous studies investigating global metabolomics in *Salmonella* infections have focused on the hosts with conventional mouse microbiota, finding disruptions in host hormone pathways (51), changes in common microbial metabolites, including trimethylamine *N*-oxide (TMAO) and hippurate (52), and changes in sugar moieties (43). Our study differed from these previous studies in that we used gnotobiotic mice to specifically focus on metabolites produced when human-associated gut microbiota strains were exposed to pathogens. While using native microbiota to look for pathogen interactions is valuable especially in an ecological context, the humanized mouse model enables exploration of potentially distinct chemical interactions between human microbiota strains and human pathogens (53). Furthermore, human gut microbiota extracts have been previously shown to inhibit virulence of *Salmonella in vitro* (40). Mice monocolonized with pathogens serve as key controls that allowed us to focus on compounds apparently made by the microbiota during infection rather than overall host changes. Nevertheless, the possibility exists that we may detect metabolites made by *Salmonella* in response to gut microbiota in our experiments or metabolites that differ due to GF mice exhibiting colitis rather than the typical systemic typhoid-like infection (54). In addition, we scanned for molecular features with an *m/z* greater than 200, to avoid discovery of smaller commonly made microbial metabolites. In our metabolites of interest from humanized infection conditions, we had many molecular features that were not identified with KEGG, HMDB, or AntiBase, potentially indicating novel metabolites. One drawback in studying these metabolite interactions *in vivo* is the challenge in isolating individual novel molecules from a complex mixture, even in a well-described community with full genomes (55), as we were unable to match known and predicted metabolites to a majority of our target *m/z* values. Although work is being done to increase MS/MS databases for natural products (56), identifying natural products is still challenging, as many natural product databases, including AntiBase, are not MS compatible.

We were able to identify a few metabolites specific to the humanized *Salmonella*-infected group, including two metabolites in the glutathione pathway. In particular, we identified glutathione disulfide and glutathione cysteine disulfide in higher abundance in humanized *Salmonella*-infected mice. *Salmonella* infection triggers vast amounts of oxidative stress (57), and glutathione metabolism is important for protection against oxidative stress (58). Changes in genes encoding antioxidant proteins have also been identified in humans exposed to *Salmonella enterica* serovar Typhi (59). Further, glutathione cysteine disulfide has been shown to reduce colonic lesions in a mouse model of colitis (60). Previous work indicates that germfree mice have a disrupted glutathione metabolism relative to conventional mice (61). It remains to be seen whether experimentally manipulating glutathione metabolite amounts affects *Salmonella* infections *in vivo*, and to what extent different gut microbes contribute to the glutathione pool. In contrast to the hypothesis that microbes may make specific metabolites that inhibit certain pathogens, this evidence suggests more generalized responses to certain kinds of dysbiosis, such as oxidative stress (62). The possibility of microbial metabolites with specific responses to pathogens cannot be eliminated; however, many metabolites remain unidentified, and the roles of those identified are unclear. Further characterization of microbial metabolites made during infection is necessary to identify these responses.

Colonization resistance conferred by the microbiota helps the host resist a variety of pathogens, including *Salmonella*. Understanding the complex interactions between the host, microbiota, and pathogens will enable better microbiome based-therapies, from fecal microbiota transplants to microbiota-derived compounds (63, 64). Combining gnotobiotic mice with genomics and metabolomics has allowed us to interrogate changes in community composition and function during infection in an unbiased

manner and demonstrates distinct metabolic responses to a virulent or opportunistic pathogen.

MATERIALS AND METHODS

Human gut microbiota and pathogens. For our synthetic human microbiome gut community, we used a collection of previously obtained isolates cultured from human fecal samples and maintained in long-term storage in the Rey lab at the University of Wisconsin-Madison. Bacterial isolates (Table S3) were grown from glycerol stock on Mega Medium (65), which was filter sterilized and held in a Coy anaerobic chamber (5% H_2, 20% CO_2, and 75% N_2). An even mix from each bacterial culture was inoculated into each anaerobic tube. From stock cultures, *Salmonella enterica* Typhimurium ATCC 14028 was grown aerobically overnight in LB broth at 37°C, while *Candida albicans* K1 was grown on Sabouraud dextrose agar (SDA).

Gnotobiotic mice and experimental infections. The University of Wisconsin-Madison Animal Care and Use Committee approved protocols used in mouse experiments. GF male C57BL/6J mice were maintained in gnotobiotic isolators until 8 to 12 weeks of age with 12-h light cycle and sterilized food and water *ad libitum*. These GF mice were then randomly assigned to 1 of 5 treatment groups, moved to out-of-the-isolator gnotobiotic cages in autoclaved filter-top cages, and subsequently gavaged in a biosafety cabinet using aseptic technique (66). Mice were housed 3 per cage, with a total of 6 mice per group.

To humanize mice, GF mice were colonized via oral gavage with 0.2 ml mixed bacterial culture as shown in Table S3. All HUM mice were given the same inoculum, where bacteria were mixed with roughly similar proportions. Prior to infection, HUM mice were given 2 weeks to allow stabilization of the community. For mouse infections, mice were inoculated via oral gavage with 0.2 ml of overnight culture of *Salmonella enterica* Typhimurium ATCC 14028 or *Candida albicans* K1. Humanization and infection treatments were performed in a biosafety cabinet using aseptic technique (66). Mice were sacrificed 3 days postinfection or earlier depending on symptom severity and weight loss. Cecal contents were collected, flash frozen and stored at −80°C until processing. We selected cecum contents for LC-MS due to their high microbial loads and proximity to the distal ileum to which *Salmonella* localizes (28, 67).

Salmonella and *Candida* quantification was performed by serial dilutions of fecal samples in phosphate-buffered saline, followed by plating for quantification for *Salmonella* on xylose lysine deoxycholate (XLD) agar, and for *Candida* on SDA with chloramphenicol and gentamicin. Fecal samples from uninfected mice showed no growth on the SDA plates, as well as no growth of black colonies on XLD plates, indicating no colonies capable of metabolizing thiosulfate into hydrogen sulfide as *Salmonella* does.

Metagenomics. To characterize the gut microbiome of HUM mice, we conducted metagenomics using Illumina MiSeq. Genomic DNA was extracted from fecal pellets following the Turnbaugh et al. protocol (68). Briefly, the protocol is as follows: to each frozen fecal pellet, we added 500 μl of extraction buffer (200 mM Tris, 200 nM NaCl, 20 mM EDTA), 210 μl 20% SDS, 500 μl phenol-chloroform, 500 μl 0.1-mm zirconia-silica beads, and one 3.2-mm stainless steel bead. Cells were beaten for 3 min at room temperature. To remove contaminants, the Wizard SV Gel and PCR Clean-up kit was used. DNA library preparation and sequencing were done at the University of Wisconsin-Madison Biotechnology Center. Samples were prepared with the TruSeq Nano DNA LT Library Prep kit (Illumina Inc., San Diego, CA, USA) with minor modifications. After shearing samples with a Covaris M220 Ultrasonicator (Covaris Inc., Woburn, MA, USA), samples were size selected for an average insert size of 550 bp using SPRI bead-based size exclusion, and then libraries were standardized to 2 nM. Sequencing was done using single ends on the Illumina MiSeq sequencer with a 50-bp (v2) sequencing cartridge.

Metagenomic data were preprocessed using BBDuk (https://sourceforge.net/projects/bbmap/) to trim adapters, remove phi-X contamination, and quality trim reads to Q10. We analyzed the reads using the COPROseq (Community profiling by sequencing) pipeline (69), which mapped reads to reference genomes using Bowtie version 1.0 (70), and normalized reads based on genome length. We also compared read mapping using the Burrows-Wheeler Alignment tool to verify that reads mapped consistently (71). Reference genomes were obtained from NCBI. Diversity was analyzed using the vegan package in R with a Kruskal-Wallis test. Biosynthetic gene clusters were identified using antiSMASH 4.0 (37). Gene clusters were then grouped by similarity using BiG-SCAPE (J. Navarro-Muñoz et al., unpublished data; https://git.wageningenur.nl/medema-group/BiG-SCAPE). Data were analyzed and figures produced in R. Statistical testing was done using a Wilcoxon rank sum test (Mann-Whitney U test) with a Benjamini-Hochberg correction.

Metabolomics. All chemicals were obtained from Fisher Scientific unless otherwise noted. Mouse cecum samples were placed in 10-ml PTFE tubes for extraction with a methanol-chloroform/water extraction. Three parts methanol, 1 part chloroform, and 4 parts water (Milli-Q system, Millipore, Billerica, MA) were added, in order, to each sample (total volume, 4 ml) and centrifuged for 20 min at 4,575 × *g* at 4°C. The aqueous fraction was removed, and 4 parts methanol were then added. After brief vortexing, samples were centrifuged for 5 min at 1,500 × *g* and 4°C. The organic layer was removed. Samples were dried in a SpeedVac and stored at −80°C. To clean up the sample, the aqueous fraction was further processed with a 3-kDa molecular weight cutoff (MWCO) (Amicon Ultra, Millipore). The MWCO device was rinsed with 0.2 ml 0.1 M NaOH and 0.5 ml 50/50 methanol-water. The sample was loaded in 0.5 ml 50/50 methanol-water and rinsed with 0.1 ml 50/50 methanol-water. All centrifugations occurred at 14,000 × *g* until the rinse or sample was through the device. The MWCO flowthrough was dried with a SpeedVac and stored at −80°C until analysis.

Aqueous samples were resuspended in optima-grade water at a concentration of 10 mg/ml. A Dionex Ultimate 3000 UHPLC system (Thermo Scientific, Waltham, MA, USA) and a Cortecs C_{18} column (2.1-mm internal diameter × 100-mm length, 1.6-μm particle size; Waters, Milford, MA, USA), equipped with a corresponding guard column were used to separate the samples. The column temperature was 35°C, and the mobile phases were optima-grade water with 0.1% formic acid (A) and acetonitrile with 0.1% formic acid (B). The separation occurred with a 35-min gradient at a flow rate of 0.3 ml/minutes with the following conditions: 0 to 5 min, 1% B; 5 to 10 min, linear gradient from 1% to 3% B; 10 to 18 min, linear gradient from 3% to 40% B; 18 to 22 min, linear gradient from 40% to 80% B; 22 to 27 min, column cleaning at 95% B; and 27 to 35 min, reequilibration at 1% B. The injection volume was 3 μl and the samples were kept at 10°C during analysis. Metabolite MS data were acquired on a Q-Exactive Orbitrap mass spectrometer (Thermo Scientific, Waltham, MA, USA), which was equipped with an ESI source and operated in positive ion mode with a scan range of *m/z* 200 to 1,700. The MS parameters were as follows: 70,000 resolution, 1E6 AGC, and 100-ms maximum injection time.

Metabolomics data analysis. Relative quantification of the metabolomics data for the different sample types was performed with Compound Discoverer software (Thermo Scientific, Waltham, MA, USA). Spectra underwent retention time alignment (adaptive curve 5 ppm, 1-min tolerances), detection of unknown compounds (5 ppm, 30 intensity threshold, 3 S/N threshold, 1,000,000 minimum peak intensity), and grouping of unknown compounds (5 ppm, 0.05 retention time tolerance). The Compound Discoverer workflow also included fill gaps, mark background, predict compositions, ChemSpider search, normalize areas (constant sum), merge features, and differential analysis. To isolate metabolites of interest, *m/z* values detected in the blanks or in more than 4 of 12 replicates in either of the germfree infected conditions were removed. Additionally, *m/z* were selected if they showed 1.5-fold upregulation in 8 of 12 replicates of the infected humanized group, with the ratios being calculated from the control with the highest normalized area. MetaboAnalyst (72, 73) was used for further statistical analysis after exporting *m/z* values, retention time, and normalized areas from Compound Discoverer. Data were filtered with an interquantile range (IQR) estimate and log transformed. Heatmaps were produced using Pearson and Ward clustering.

Compound identification. MS/MS spectra for the compounds on the target lists for both infections were collected on the Dionex UltiMate 3000 UHPLC and Q-Exactive instrument described above. The injection volume was 20 μl. An inclusion list was used for the targets with a retention time window of ± 0.7 min. All charge states and salt adducts observed in the Compound Discoverer analysis were included in the inclusion list. The MS^2 parameters were as follows: 70,000 resolution, 5 E5 AGC, 100-ms maximum injection time, 1.0 *m/z* isolation window, and 30 NCE. MetFrag *in silico* fragmentation prediction software was used to aid in metabolite identification (38). Target molecules were searched against KEGG and PubChem databases with a 5-ppm error. Candidate molecules from the databases were then processed against the MS/MS spectra of the target molecule with 5-ppm and 0.01-m/zabs settings. The top results of the *in silico* fragmentation were analyzed for putative identification. Putative identifications were then verified by comparing the experimental MS/MS to the MS/MS of the commercial standard.

Accession number(s). The metagenome sequences from this study are available under the BioProject identifier PRJNA491522 (https://www.ncbi.nlm.nih.gov/sra/PRJNA491522). The metabolomics data are available from the MetaboLights database under the accession number MTBLS753 (https://www.ebi.ac.uk/metabolights/MTBLS753).

SUPPLEMENTAL MATERIAL

Supplemental material for this article may be found at https://doi.org/10.1128/mBio.02032-18.

FIG S1, EPS file, 0.8 MB.
FIG S2, EPS file, 2.7 MB.
FIG S3, EPS file, 3.2 MB.
FIG S4, EPS file, 2.4 MB.
TABLE S1, DOCX file, 0.01 MB.
TABLE S2, DOCX file, 0.01 MB.
TABLE S3, DOCX file, 0.02 MB.

ACKNOWLEDGMENTS

This work was supported by T32AI55397 and U19AI109673 from the National Institutes of Health, and the Office of the Vice Chancellor for Research and Graduate Education at the University of Wisconsin–Madison with funding from the Wisconsin Alumni Research Foundation. Sequencing was provided by the University of Wisconsin Biotech Center. This work was supported in part by grants NIH DK108259 (to F.E.R.). L.L. acknowledges a Vilas Distinguished Achievement Professorship, NIH DK071801, and S10RR029531. The Q-Exactive instrument was purchased through an NIH shared instrument grant (NCRR S10RR029531).

We thank Kimberley Romano for assistance in mouse experimental procedures and Marc Chevrette for advice on secondary metabolite clustering methods. We also thank

Camila Carlos, Lily Khadempour, Heidi Horn, and Lindsay Kalan for critical feedback on the manuscript.

REFERENCES

1. Phane Hacquard S, Garrido-Oter R, Gonzá A, Spaepen S, Ackermann G, Lebeis S, McHardy AC, Dangl JL, Knight R, Ley R, Schulze-Lefert P. 2015. Microbiota and host nutrition across plant and animal kingdoms. Cell Host Microbe 17:603–616. https://doi.org/10.1016/j.chom.2015.04.009.
2. Sharon G, Garg N, Debelius J, Knight R, Dorrestein PC, Mazmanian SK. 2014. Specialized metabolites from the microbiome in health and disease. Cell Metab 20:719–730. https://doi.org/10.1016/j.cmet.2014.10.016.
3. Lynch SV, Pedersen O. 2016. The human intestinal microbiome in health and disease. N Engl J Med 375:2369–2379. https://doi.org/10.1056/NEJMra1600266.
4. Sender R, Fuchs S, Milo R. 2016. Revised estimates for the number of human and bacteria cells in the body. PLoS Biol 14:e1002533. https://doi.org/10.1371/journal.pbio.1002533.
5. Walter J, Ley R. 2011. The human gut microbiome: ecology and recent evolutionary changes. Annu Rev Microbiol 65:411–429. https://doi.org/10.1146/annurev-micro-090110-102830.
6. Scanlan PD, Marchesi JR. 2008. Micro-eukaryotic diversity of the human distal gut microbiota: qualitative assessment using culture-dependent and -independent analysis of faeces. ISME J 2:1183–1193. https://doi.org/10.1038/ismej.2008.76.
7. Hoffmann C, Dollive S, Grunberg S, Chen J, Li H, Wu GD, Lewis JD, Bushman FD. 2013. Archaea and fungi of the human gut microbiome: correlations with diet and bacterial residents. PLoS One 8:e66019. https://doi.org/10.1371/annotation/31412345-fc86-4d67-b37c-93d42f5f0a59.
8. Minot S, Sinha R, Chen J, Li H, Keilbaugh SA, Wu GD, Lewis JD, Bushman FD. 2011. The human gut virome: inter-individual variation and dynamic response to diet. Genome Res 21:1616–1625. https://doi.org/10.1101/gr.122705.111.
9. Qin J, Li R, Raes J, Arumugam M, Burgdorf KS, Manichanh C, Nielsen T, Pons N, Levenez F, Yamada T, Mende DR, Li J, Xu J, Li S, Li D, Cao J, Wang B, Liang H, Zheng H, Xie Y, Tap J, Lepage P, Bertalan M, Batto J-M, Hansen T, Le Paslier D, Linneberg A, Nielsen HB, Pelletier E, Renault P, Sicheritz-Ponten T, Turner K, Zhu H, Yu C, Li S, Jian M, Zhou Y, Li Y, Zhang X, Li S, Qin N, Yang H, Wang J, Brunak S, Doré J, Guarner F, Kristiansen K, Pedersen O, Parkhill J, Weissenbach J, Bork P, Ehrlich SD, Wang J. 2010. A human gut microbial gene catalogue established by metagenomic sequencing. Nature 464:59–65. https://doi.org/10.1038/nature08821.
10. Lloyd-Price J, Mahurkar A, Rahnavard G, Crabtree J, Orvis J, Hall AB, Brady A, Creasy HH, McCracken C, Giglio MG, McDonald D, Franzosa EA, Knight R, White O, Huttenhower C. 2017. Strains, functions and dynamics in the expanded Human Microbiome Project. Nature 550:61. https://doi.org/10.1038/nature23889.
11. Faith JJ, Guruge JL, Charbonneau M, Subramanian S, Seedorf H, Goodman AL, Clemente JC, Knight R, Heath AC, Leibel RL, Rosenbaum M, Gordon JI. 2013. The long-term stability of the human gut microbiota. Science 341:1237439. https://doi.org/10.1126/science.1237439.
12. Buffie CG, Jarchum I, Equinda M, Lipuma L, Gobourne A, Viale A, Ubeda C, Xavier J, Pamer EG. 2012. Profound alterations of intestinal microbiota following a single dose of clindamycin results in sustained susceptibility to Clostridium difficile-induced colitis. Infect Immun 80:62–73. https://doi.org/10.1128/IAI.05496-11.
13. Ubeda C, Taur Y, Jenq RR, Equinda MJ, Son T, Samstein M, Viale A, Socci ND, van den Brink MRM, Kamboj M, Pamer EG. 2010. Vancomycin-resistant Enterococcus domination of intestinal microbiota is enabled by antibiotic treatment in mice and precedes bloodstream invasion in humans. J Clin Invest 120:4332–4341. https://doi.org/10.1172/JCI43918.
14. Lawley TD, Bouley DM, Hoy YE, Gerke C, Relman DA, Monack DM. 2008. Host transmission of Salmonella enterica serovar Typhimurium is controlled by virulence factors and indigenous intestinal microbiota. Infect Immun 76:403–416. https://doi.org/10.1128/IAI.01189-07.
15. Bohnhoff M, Drake BL, Miller CP. 1954. Effect of streptomycin on susceptibility of intestinal tract to experimental Salmonella infection. Proc Soc Exp Biol Med 86:132–137. https://doi.org/10.3181/00379727-86-21030.
16. Buffie CG, Pamer EG. 2013. Microbiota-mediated colonization resistance against intestinal pathogens. Nat Rev Immunol 13:790–801. https://doi.org/10.1038/nri3535.
17. Spees AM, Lopez CA, Kingsbury DD, Winter SE, Bäumler AJ. 2013. Colonization resistance: battle of the bugs or ménage à trois with the host? PLoS Pathog 9:e1003730. https://doi.org/10.1371/journal.ppat.1003730.
18. Steed AL, Christophi GP, Kaiko GE, Sun L, Goodwin VM, Jain U, Esaulova E, Artyomov MN, Morales DJ, Holtzman MJ, Boon ACM, Lenschow DJ, Stappenbeck TS. 2017. The microbial metabolite desaminotyrosine protects from influenza through type I interferon. Science 357:498–502. https://doi.org/10.1126/science.aam5336.
19. Buffie CG, Bucci V, Stein RR, McKenney PT, Ling L, Gobourne A, No D, Liu H, Kinnebrew M, Viale A, Littmann E, van den Brink MRM, Jenq RR, Taur Y, Sander C, Cross JR, Toussaint NC, Xavier JB, Pamer EG. 2015. Precision microbiome reconstitution restores bile acid mediated resistance to Clostridium difficile. Nature 517:205–208. https://doi.org/10.1038/nature13828.
20. Hsiao A, Ahmed AMS, Subramanian S, Griffin NW, Drewry LL, Petri WA, Haque R, Ahmed T, Gordon JI, Gordon JI. 2014. Members of the human gut microbiota involved in recovery from Vibrio cholerae infection. Nature 515:423–426. https://doi.org/10.1038/nature13738.
21. Donia MS, Cimermancic P, Schulze CJ, Wieland Brown LC, Martin J, Mitreva M, Clardy J, Linington RG, Fischbach MA. 2014. A systematic analysis of biosynthetic gene clusters in the human microbiome reveals a common family of antibiotics. Cell 158:1402–1414. https://doi.org/10.1016/j.cell.2014.08.032.
22. Claus SP, Tsang TM, Wang Y, Cloarec O, Skordi E, Martin F-P, Rezzi S, Ross A, Kochhar S, Holmes E, Nicholson JK. 2008. Systemic multicompartmental effects of the gut microbiome on mouse metabolic phenotypes. Mol Syst Biol 4:219. https://doi.org/10.1038/msb.2008.56.
23. Martin F-PJ, Dumas M-E, Wang Y, Legido-Quigley C, Yap IKS, Tang H, Zirah S, Murphy GM, Cloarec O, Lindon JC, Sprenger N, Fay LB, Kochhar S, van Bladeren P, Holmes E, Nicholson JK. 2007. A top-down systems biology view of microbiome-mammalian metabolic interactions in a mouse model. Mol Syst Biol 3:112. https://doi.org/10.1038/msb4100153.
24. Zheng X, Xie G, Zhao A, Zhao L, Yao C, Chiu NHL, Zhou Z, Bao Y, Jia W, Nicholson JK, Jia W. 2011. The footprints of gut microbial–mammalian co-metabolism. J Proteome Res 10:5512–5522. https://doi.org/10.1021/pr2007945.
25. Lu K, Abo RP, Schlieper KA, Graffam ME, Levine S, Wishnok JS, Swenberg JA, Tannenbaum SR, Fox JG. 2014. Arsenic exposure perturbs the gut microbiome and its metabolic profile in mice: an integrated metagenomics and metabolomics analysis. Environ Health Perspect 122:284–291. https://doi.org/10.1289/ehp.1307429.
26. Hou Y, Braun DR, Michel CR, Klassen JL, Adnani N, Wyche TP, Bugni TS. 2012. Microbial strain prioritization using metabolomics tools for the discovery of natural products. Anal Chem 84:4277–4283. https://doi.org/10.1021/ac202623g.
27. Krug D, Zurek G, Revermann O, Vos M, Velicer GJ, Müller R. 2008. Discovering the hidden secondary metabolome of Myxococcus xanthus: a study of intraspecific diversity. Appl Environ Microbiol 74:3058–3068. https://doi.org/10.1128/AEM.02863-07.
28. Barman M, Unold D, Shifley K, Amir E, Hung K, Bos N, Salzman N. 2008. Enteric salmonellosis disrupts the microbial ecology of the murine gastrointestinal tract. Infect Immun 76:907–915. https://doi.org/10.1128/IAI.01432-07.
29. Stecher B, Robbiani R, Walker AW, Westendorf AM, Barthel M, Kremer M, Chaffron S, Macpherson AJ, Buer J, Parkhill J, Dougan G, von Mering C, Hardt W-D. 2007. Salmonella enterica serovar Typhimurium exploits inflammation to compete with the intestinal microbiota. PLoS Biol 5:e244. https://doi.org/10.1371/journal.pbio.0050244.
30. Rivera-Chávez F, Bäumler AJ. 2015. The pyromaniac inside you: *Salmonella* metabolism in the host gut. Annu Rev Microbiol 69:31–48. https://doi.org/10.1146/annurev-micro-091014-104108.
31. Kumamoto CA. 2011. Inflammation and gastrointestinal Candida colonization. Curr Opin Microbiol 14:386–391. https://doi.org/10.1016/j.mib.2011.07.015.

32. Mason KL, Erb Downward JR, Falkowski NR, Young VB, Kao JY, Huffnagle GB. 2012. Interplay between the gastric bacterial microbiota and Candida albicans during postantibiotic recolonization and gastritis. Infect Immun 80:150–158. https://doi.org/10.1128/IAI.05162-11.
33. Koh AY. 2013. Murine models of Candida gastrointestinal colonization and dissemination. Eukaryot Cell 12:1416–1422. https://doi.org/10.1128/EC.00196-13.
34. Auchtung TA, Fofanova TY, Stewart CJ, Nash AK, Wong MC, Gesell JR, Auchtung JM, Ajami NJ, Petrosino JF. 2018. Investigating colonization of the healthy adult gastrointestinal tract by fungi. mSphere 3:e00092-18. https://doi.org/10.1128/mSphere.00092-18.
35. Schofield DA, Westwater C, Balish E. 2005. Divergent chemokine, cytokine and -defensin responses to gastric candidiasis in immunocompetent C57BL/6 and BALB/c mice. J Med Microbiol 54:87–92. https://doi.org/10.1099/jmm.0.45755-0.
36. Kennedy MJ, Volz PA. 1985. Effect of various antibiotics on gastrointestinal colonization and dissemination by *Candida albicans*. Med Mycol 23:265–273. https://doi.org/10.1080/00362178585380391.
37. Blin K, Wolf T, Chevrette MG, Lu X, Schwalen CJ, Kautsar SA, Suarez Duran HG, de los Santos ELC, Kim HU, Nave M, Dickschat JS, Mitchell DA, Shelest E, Breitling R, Takano E, Lee SY, Weber T, Medema MH. 2017. antiSMASH 4.0—improvements in chemistry prediction and gene cluster boundary identification. Nucleic Acids Res 45:W36–W41. https://doi.org/10.1093/nar/gkx319.
38. Ruttkies C, Schymanski EL, Wolf S, Hollender J, Neumann S. 2016. MetFrag relaunched: incorporating strategies beyond in silico fragmentation. J Cheminform 8:3. https://doi.org/10.1186/s13321-016-0115-9.
39. Costello EK, Stagaman K, Dethlefsen L, Bohannan BJM, Relman DA. 2012. The application of ecological theory toward an understanding of the human microbiome. Science 336:1255–1262. https://doi.org/10.1126/science.1224203.
40. Antunes LCM, McDonald JAK, Schroeter K, Carlucci C, Ferreira RBR, Wang M, Yurist-Doutsch S, Hira G, Jacobson K, Davies J, Allen-Vercoe E, Finlay BB. 2014. Antivirulence activity of the human gut metabolome. mBio 5:e01183-14. https://doi.org/10.1128/mBio.01183-14.
41. Byrd AL, Segre JA. 2016. Criteria for disease causation must take microbial interactions into account. Science 351:224–226. https://doi.org/10.1126/science.aad6753.
42. Wesolowska-Andersen A, Bahl MI, Carvalho V, Kristiansen K, Sicheritz-Pontén T, Gupta R, Licht TR. 2014. Choice of bacterial DNA extraction method from fecal material influences community structure as evaluated by metagenomic analysis. Microbiome 2:19. https://doi.org/10.1186/2049-2618-2-19.
43. Deatherage Kaiser BL, Li J, Sanford JA, Kim Y-M, Kronewitter SR, Jones MB, Peterson CT, Peterson SN, Frank BC, Purvine SO, Brown JN, Metz TO, Smith RD, Heffron F, Adkins JN. 2013. A multi-omic view of host-pathogen-commensal interplay in Salmonella-mediated intestinal infection. PLoS One 8:e67155. https://doi.org/10.1371/journal.pone.0067155.
44. Stecher B, Chaffron S, Käppeli R, Hapfelmeier S, Freedrich S, Weber TC, Kirundi J, Suar M, McCoy KD, von Mering C, Macpherson AJ, Hardt W-D. 2010. Like will to like: abundances of closely related species can predict susceptibility to intestinal colonization by pathogenic and commensal bacteria. PLoS Pathog 6:e1000711. https://doi.org/10.1371/journal.ppat.1000711.
45. Rivera-Chávez F, Lopez CA, Bäumler AJ. 2017. Oxygen as a driver of gut dysbiosis. Free Radic Biol Med 105:93–101. https://doi.org/10.1016/j.freeradbiomed.2016.09.022.
46. Thiennimitr P, Winter SE, Winter MG, Xavier MN, Tolstikov V, Huseby DL, Sterzenbach T, Tsolis RM, Roth JR, Bäumler AJ. 2011. Intestinal inflammation allows Salmonella to use ethanolamine to compete with the microbiota. Proc Natl Acad Sci U S A 108:17480–17485. https://doi.org/10.1073/pnas.1107857108.
47. Deriu E, Liu JZ, Pezeshki M, Edwards RA, Ochoa RJ, Contreras H, Libby SJ, Fang FC, Raffatellu M. 2013. Probiotic bacteria reduce Salmonella Typhimurium intestinal colonization by competing for iron. Cell Host Microbe 14:26–37. https://doi.org/10.1016/j.chom.2013.06.007.
48. Letzel A-C, Pidot SJ, Hertweck C. 2013. A genomic approach to the cryptic secondary metabolome of the anaerobic world. Nat Prod Rep 30:392–428. https://doi.org/10.1039/C2NP20103H.
49. Just-Baringo X, Albericio F, Álvarez M. 2014. Thiopeptide antibiotics: retrospective and recent advances. Mar Drugs 12:317–351. https://doi.org/10.3390/md12010317.
50. Marcobal A, Kashyap PC, Nelson TA, Aronov PA, Donia MS, Spormann A, Fischbach MA, Sonnenburg JL. 2013. A metabolomic view of how the human gut microbiota impacts the host metabolome using humanized and gnotobiotic mice. ISME J 7:1933–1943. https://doi.org/10.1038/ismej.2013.89.
51. Antunes LCM, Arena ET, Menendez A, Han J, Ferreira RBR, Buckner MMC, Lolic P, Madilao LL, Bohlmann J, Borchers CH, Finlay BB. 2011. Impact of salmonella infection on host hormone metabolism revealed by metabolomics. Infect Immun 79:1759–1769. https://doi.org/10.1128/IAI.01373-10.
52. Zhu X, Lei H, Wu J, Li JV, Tang H, Wang Y. 2014. Systemic responses of BALB/c mice to *Salmonella typhimurium* Infection. J Proteome Res 13:4436–4445. https://doi.org/10.1021/pr500770x.
53. Arrieta M-C, Walter J, Finlay BB. 2016. Human microbiota-associated mice: a model with challenges. Cell Host Microbe 19:575–578. https://doi.org/10.1016/j.chom.2016.04.014.
54. Stecher B, Macpherson AJ, Hapfelmeier S, Kremer M, Stallmach T, Hardt W-D. 2005. Comparison of Salmonella enterica serovar Typhimurium colitis in germfree mice and mice pretreated with streptomycin. Infect Immun 73:3228–3241. https://doi.org/10.1128/IAI.73.6.3228-3241.2005.
55. Li JW-H, Vederas JC. 2009. Drug discovery and natural products: end of an era or an endless frontier? Science 325:161–165. https://doi.org/10.1126/science.1168243.
56. Wang M, Carver JJ, Phelan VV, Sanchez LM, Garg N, Peng Y, Nguyen DD, Watrous J, Kapono CA, Luzzatto-Knaan T, Porto C, Bouslimani A, Melnik AV, Meehan MJ, Liu W-T, Crüsemann M, Boudreau PD, Esquenazi E, Sandoval-Calderón M, Kersten RD, Pace LA, Quinn RA, Duncan KR, Hsu C-C, Floros DJ, Gavilan RG, Kleigrewe K, Northen T, Dutton RJ, Parrot D, Carlson EE, Aigle B, Michelsen CF, Jelsbak L, Sohlenkamp C, Pevzner P, Edlund A, McLean J, Piel J, Murphy BT, Gerwick L, Liaw C-C, Yang Y-L, Humpf H-U, Maansson M, Keyzers RA, Sims AC, Johnson AR, Sidebottom AM, Sedio BE, Klitgaard A, Larson CB, Boya P CA, Torres-Mendoza D, Gonzalez DJ, Silva DB, Marques LM, Demarque DP, Pociute E, O'Neill EC, Briand E, Helfrich EJN, Granatosky EA, Glukhov E, Ryffel F, Houson H, Mohimani H, Kharbush JJ, Zeng Y, Vorholt JA, Kurita KL, Charusanti P, McPhail KL, Nielsen KF, Vuong L, Elfeki M, Traxler MF, Engene N, Koyama N, Vining OB, Baric R, Silva RR, Mascuch SJ, Tomasi S, Jenkins S, Macherla V, Hoffman T, Agarwal V, Williams PG, Dai J, Neupane R, Gurr J, Rodríguez AMC, Lamsa A, Zhang C, Dorrestein K, Duggan BM, Almaliti J, Allard P-M, Phapale P, Nothias L-F, Alexandrov T, Litaudon M, Wolfender J-L, Kyle JE, Metz TO, Peryea T, Nguyen D-T, VanLeer D, Shinn P, Jadhav A, Müller R, Waters KM, Shi W, Liu X, Zhang L, Knight R, Jensen PR, Palsson BO, Pogliano K, Linington RG, Gutiérrez M, Lopes NP, Gerwick WH, Moore BS, Dorrestein PC, Bandeira N. 2016. Sharing and community curation of mass spectrometry data with Global Natural Products Social Molecular Networking. Nat Biotechnol 34:828–837. https://doi.org/10.1038/nbt.3597.
57. Farr SB, Kogoma T. 1991. Oxidative stress responses in Escherichia coli and Salmonella typhimurium. Microbiol Rev 55:561–585.
58. Hayes JD, McLellan LI. 1999. Glutathione and glutathione-dependent enzymes represent a co-ordinately regulated defence against oxidative stress. Free Radic Res 31:273–300. https://doi.org/10.1080/10715769900300851.
59. Zhang Y, Brady A, Jones C, Song Y, Darton TC, Jones C, Blohmke CJ, Pollard AJ, Magder LS, Fasano A, Sztein MB, Fraser CM. 2018. Compositional and functional differences in the human gut microbiome correlate with clinical outcome following infection with wild-type Salmonella enterica serovar Typhi. mBio 9:e00686-18.
60. Oz HS, Chen TS, Nagasawa H. 2007. Comparative efficacies of 2 cysteine prodrugs and a glutathione delivery agent in a colitis model. Transl Res 150:122–129. https://doi.org/10.1016/j.trsl.2006.12.010.
61. Mardinoglu A, Shoaie S, Bergentall M, Ghaffari P, Zhang C, Larsson E, Bäckhed F, Nielsen J. 2015. The gut microbiota modulates host amino acid and glutathione metabolism in mice. Mol Syst Biol 11:834. https://doi.org/10.15252/msb.20156487.
62. Duvallet C, Gibbons SM, Gurry T, Irizarry RA, Alm EJ. 2017. Meta-analysis of gut microbiome studies identifies disease-specific and shared responses. Nat Commun 8:1784. https://doi.org/10.1038/s41467-017-01973-8.
63. Kassam Z, Lee CH, Yuan Y, Hunt RH. 2013. Fecal microbiota transplantation for Clostridium difficile infection: systematic review and meta-analysis. Am J Gastroenterol 108:500–508. https://doi.org/10.1038/ajg.2013.59.
64. Suez J, Elinav E. 2017. The path towards microbiome-based metabolite treatment. Nat Microbiol 2:17075. https://doi.org/10.1038/nmicrobiol.2017.75.
65. Romano KA, Vivas EI, Amador-Noguez D, Rey FE. 2015. Intestinal micro-

biota composition modulates choline bioavailability from diet and accumulation of the proatherogenic metabolite trimethylamine-N-oxide. mBio 6:e02481-14. https://doi.org/10.1128/mBio.02481-14.
66. Faith JJ, Ahern PP, Ridaura VK, Cheng J, Gordon JI. 2014. Identifying gut microbe-host phenotype relationships using combinatorial communities in gnotobiotic mice. Sci Transl Med 6:220ra11. https://doi.org/10.1126/scitranslmed.3008051.
67. Dunne C. 2001. Adaptation of bacteria to the intestinal niche: probiotics and gut disorder. Inflamm Bowel Dis 7:136–145. https://doi.org/10.1097/00054725-200105000-00010.
68. Turnbaugh PJ, Ridaura VK, Faith JJ, Rey FE, Knight R, Gordon JI. 2009. The effect of diet on the human gut microbiome: a metagenomic analysis in humanized gnotobiotic mice. Sci Transl Med 1:6ra14. https://doi.org/10.1126/scitranslmed.3000322.
69. McNulty NP, Yatsunenko T, Hsiao A, Faith JJ, Muegge BD, Goodman AL, Henrissat B, Oozeer R, Cools-Portier S, Gobert G, Chervaux C, Knights D, Lozupone CA, Knight R, Duncan AE, Bain JR, Muehlbauer MJ, Newgard CB, Heath AC, Gordon JI. 2011. The impact of a consortium of fermented milk strains on the gut microbiome of gnotobiotic mice and monozygotic twins. Sci Transl Med 3:106ra106. https://doi.org/10.1126/scitranslmed.3002701.
70. Langmead B, Trapnell C, Pop M, Salzberg SL. 2009. Ultrafast and memory-efficient alignment of short DNA sequences to the human genome. Genome Biol 10:R25. https://doi.org/10.1186/gb-2009-10-3-r25.
71. Li H, Durbin R. 2009. Fast and accurate short read alignment with Burrows-Wheeler transform. Bioinformatics 25:1754–1760. https://doi.org/10.1093/bioinformatics/btp324.
72. Xia J, Sinelnikov IV, Han B, Wishart DS. 2015. MetaboAnalyst 3.0—making metabolomics more meaningful. Nucleic Acids Res 43:W251–W257. https://doi.org/10.1093/nar/gkv380.
73. Xia J, Wishart DS, Xia J, Wishart DS. 2016. Using MetaboAnalyst 3.0 for comprehensive metabolomics data analysis. Curr Protoc Bioinformatics 55:14.10.1–14.10.91. https://doi.org/10.1002/cpbi.11.